

## Artemisinin Alleviates Acrylamide-Induced Peripheral Neuropathy in Rats: The Role of PI3K/AKT Pathway

**Reda A. A. Abo-Elsoud<sup>1,5</sup>, Essam Omar Ibrahim<sup>1</sup>, Eman A. Ali<sup>2,6\*</sup>, Aliaa S. A. Alafify<sup>3</sup>, Mahmoud El Tohamy<sup>4</sup>**

<sup>1</sup>Medical Physiology Department, Faculty of Medicine, Menoufia University, Menoufia, Egypt.

<sup>2</sup>Clinical Pharmacology Department, Faculty of Medicine, Menoufia University, Menoufia, Egypt.

<sup>3</sup>Anatomy and Embryology Department, Faculty of Medicine, Menoufia University, Menoufia, Egypt.

<sup>4</sup>Medical Physiology Department, Faculty of Medicine, Mansoura University, Dakahlia, Egypt.

<sup>5</sup>Medical Physiology Department, Faculty of Medicine, Menoufia National University, Menoufia, Egypt.

<sup>6</sup>Clinical Pharmacology Department, Faculty of Medicine, Menoufia National University, Menoufia, Egypt.

**Submit Date** : 27 Apr. 2025

**Revised Date** : 18 Aug. 2025

**Accept Date** : 23 Aug. 2025

### Keywords

- Peripheral neuropathy
- Acrylamide
- Artemisinin
- PI3K/AKT pathway
- MBP

### Abstract

**Background:** Acrylamide (ACR) is a known neurotoxin that induces peripheral neuropathy through oxidative stress and inflammation. Artemisinin (ART), a bioactive compound derived from *Artemisia annua*, has exhibited promising neuroprotective and anti-inflammatory properties. **Methods:** Thirty-two rats were divided equally into control, ART-only, ACR-only, and ART + ACR groups. Neurobehavioral test (hot plate latency), electrophysiological study via nerve conduction velocity (NCV), serum oxidative and inflammatory biomarkers (MDA, TAC, TNF- $\alpha$ , IL-10), and sciatic nerve histology were evaluated. PI3K/AKT gene expression was quantified via RT-PCR, and MBP protein expression was assessed immunohistochemically. **Results:** ACR administration caused marked neuropathic changes, including reduced NCV and hot plate latency, increased MDA and TNF- $\alpha$ , decreased TAC and IL-10, downregulation of PI3K/AKT expression, and histopathological degeneration of sciatic nerve. ART treatment significantly ameliorated all these parameters, restoring nerve structure and function and enhancing PI3K/AKT and MBP expression. **Conclusion:** Artemisinin exhibits protective effects against ACR-induced peripheral neuropathy, likely via its antioxidant and anti-inflammatory actions and upregulation of the PI3K/AKT signaling pathway. ART may represent a promising therapeutic candidate for ACR-induced peripheral neuropathy.

## Introduction

Peripheral neuropathy resulting from exposure to environmental neurotoxins like acrylamide (ACR) continues to pose a significant biomedical challenge due to its multifactorial pathogenesis involving oxidative stress, neuroinflammation, and axonal degeneration [1,2]. ACR, an industrial chemical and dietary by-product formed during high-temperature cooking, inhaled smoke, is a potent neurotoxicant capable of inducing sensorimotor polyneuropathy in experimental models and humans [1,3]. Chronic ACR exposure disrupts axonal transport and causes nerve fiber degeneration, leading to functional impairments and histopathological damage [4].

ACR's neurotoxicity is closely linked to oxidative stress, mitochondrial dysfunction, and neuroinflammatory responses. ACR elevates reactive oxygen species (ROS), suppresses antioxidant defenses, and promotes lipid peroxidation in neural tissue [5,6]. Additionally, the compound interferes with redox metabolism, contributing to structural and functional damage to neurons and Schwann cells [7]. Multiple studies have confirmed that ACR impairs retrograde axonal transport, destabilizes microtubules, and activates inflammatory pathways, leading to apoptosis and progressive neurodegeneration [8,9]. Recent findings highlight the critical role of the phosphatidylinositol-3-kinase/protein kinase B (PI3K/AKT) signaling cascade in neuronal survival and regeneration. This pathway is essential for mediating anti-apoptotic signals, promoting axonal growth, and restoring functional integrity in damaged neurons. Disruption of PI3K/AKT signaling is frequently observed in

neurodegenerative diseases and toxic neuropathies, suggesting its potential as a therapeutic target [10]. Artemisinin (ART), a sesquiterpene lactone isolated from *Artemisia annua*, is widely recognized for its antimalarial properties. ART is reported to scavenge free radicals and modulate cytokine expression [11]. Furthermore, ART may enhance mitochondrial function and suppress glial activation, making it a promising candidate for managing chemically induced neuropathies.

Despite emerging evidence of ART's neuroprotective potential, limited data exist on its efficacy in counteracting ACR-induced peripheral neuropathy. Moreover, its influence on the PI3K/AKT pathway in this context remains largely unexplored. Therefore, the present study was designed to assess the neuroprotective effects of artemisinin against ACR-induced peripheral neuropathy in adult male rats. This study also aimed to evaluate behavioral, biochemical, electrophysiological, histopathological, and molecular changes, emphasizing the modulation of the PI3K/AKT signaling axis.

## Materials and Methods

### Animals

Thirty-two adult male Wistar rats weighing 200–250 g were obtained from the Experimental Animal House of the Faculty of Medicine, Menoufia University, Egypt. All procedures were conducted in accordance with the Public Health Service Policy on Humane Care and Use of Laboratory Animals and ARRIVE guidelines. Also, we gained approval from the Institutional Ethics Committee of the Faculty of Medicine, Menoufia University (Approval No.: 7/2025 PHYS 17).

## Experimental Design

### Sample size estimation

Employing the Resource Equation Method for estimating the maximum population of rats ( $n = 20/(K + 1)$ ), the sample size per group is raised from 6 to 8 rats to mitigate the dropout rate.  $k$  = the number of groups,  $n$  = the number of animals per group [12].

### Randomization and Allocation Concealment

Randomization was executed via a sequence created by Excel (v.365) by an independent researcher not engaged in data collection. Allocation concealment was preserved using sequentially numbered, opaque, sealed envelopes, which were opened solely after the enrolment of animals and completion of baseline tests to avert bias. Treatment administrators were not granted access to randomization lists during assignments. Rats were randomly allocated and divided into four equal groups ( $n = 8$  per group) as follows:

1. **Control group:** Received 0.5% carboxymethyl cellulose (CMC) and distilled water orally by gavage for 30 days.
2. **Artemisinin (ART) group:** Received ART (75 mg/kg, dissolved in 0.5% CMC), Sigma-Aldrich Chemical Company (St. Louis, MO, USA), by oral gavage three times daily for 30 days [13]. Previous research has proved the antioxidant and anti-inflammatory effects of the selected ART (75 mg/kg) dose [13].
3. **Acrylamide (ACR) group:** Received ACR (20 mg/kg, dissolved in distilled water), Sigma-Aldrich Chemical Company (St. Louis, MO, USA), by oral gavage once daily for 30 days [14]. This dose

reproduces neuropathic endpoints (NCV decline, oxidative stress, and inflammation) [14]. The Oral route was chosen as it mimics human cumulative exposure to acrylamide, resulting in peripheral neuropathy [15].

4. **Artemisinin + Acrylamide (ART + ACR) group:** Co-administered ACR and ART at the same respective doses and routes used in the ACR and ART groups for 30 consecutive days.

At the end of the experimental period, all animals underwent neurobehavioral and electrophysiological evaluations followed by blood sampling, tissue collection, and biochemical, molecular, and histological analyses.

### Blinding Procedures

All outcome evaluations utilized stringent blinding procedures:

- (a) A blinded investigator conducted behavioral and electrophysiological assessments utilizing coded animal identifiers.
- (b) Biochemical analyses employed randomized batches with laboratory personnel oblivious to group codes.
- (c) Histopathological evaluations were conducted by a pathologist unaware of the experimental settings.

### Hot Plate Latency Test

This test was used to assess acute thermal pain sensitivity. Each rat was placed at the center of a hot plate surface maintained at 52°C (Hotplate 602001; TSE Systems) within a transparent glass cylinder. The latency to paw licking or jumping was recorded as a pain response. A 30-second cut-off was applied to prevent thermal injury. The latency period was measured from the time of

placement on the plate to the first observed reaction [16].

#### **Nerve Conduction Velocity (NCV).**

Rats were anesthetized via intraperitoneal injection of xylazine HCl (10 mg/kg) and ketamine HCl (80 mg/kg)[17]. With the rat positioned prone and hind limbs extended, hair was shaved from the lower back and hind limbs. Electrical stimuli were applied using bipolar electrodes. Recording electrodes were inserted into the calf muscle. A reference electrode was placed on the untested lower limb or on the tail base [18]. The latency difference between proximal and distal stimulations was used to calculate nerve conduction velocity (NCV) using the formula:

**NCV = Distance / (Proximal latency – Distal latency)[19].**

#### **Biochemical Analysis**

After overnight fasting, retro-orbital blood samples were collected under light anesthesia. Serum was separated and analyzed for:

- **Pro-inflammatory markers:** tumor necrosis factor- $\alpha$  (TNF- $\alpha$ ) and interleukin 10 (IL-10), using ELISA kits (MyBioSource Inc., San Diego, CA, USA), following the manufacturer's instructions.
- **Oxidative stress biomarkers:** Malondialdehyde (MDA) and total antioxidant capacity (TAC), using colorimetric assay kits from Abcam (Cambridge, UK), according to the manufacturer's protocols.

#### **Quantitative Analysis of PI3K and AKT**

##### **Gene Expression by RT-PCR**

Sciatic nerve samples were isolated and immediately preserved at  $-80^{\circ}\text{C}$ . Total RNA was

extracted using the RNeasy Plus Universal Kit (Qiagen, USA). RNA integrity and purity were confirmed spectrophotometrically.

First-strand complementary DNA (cDNA) synthesis was performed using the QuantiTect Reverse Transcription Kit (Qiagen, USA) in an Applied Biosystems 2720 thermal cycler (Singapore). GAPDH was used as the reference gene.

Quantitative real-time PCR (qRT-PCR) was performed using the SensiFAST SYBR Lo-ROX Kit (USA) and Applied Biosystems 7500 software (version 2.0.1). The following primer sequences (Midland, Texas, USA) were used:

- **PI3K:**

Forward: 5'-AGC TGG TCT TCG TTT CCT GA-3'

Reverse: 5'-GAA ACT TTT TCC CAC CAC GA-3'

- **AKT:**

Forward: 5'-ATG TCC GAG ATC CTA CCC TAC G-3'

Reverse: 5'-AGC GAA GAA GGA GTT GGT GTC-3'

Relative gene expression was calculated using the comparative  $\Delta\Delta\text{Ct}$  method, with normalization to GAPDH.

#### **Histopathological and Immunohistochemical Studies**

Sciatic nerves were fixed in 10% neutral-buffered formalin, embedded in paraffin, and sectioned at 5  $\mu\text{m}$ . Sections were subjected to H&E light microscopic evaluation and immunohistochemical (IHC) assessment.

Following deparaffinization, sections were rinsed in 0.01 mol/L PBS and incubated in citrate buffer.

Endogenous peroxidase activity was blocked using 0.3% hydrogen peroxide.

Non-specific binding was blocked using 3% bovine serum albumin (BSA) at 37°C for 1 hour. Sections were incubated overnight at 4°C with the primary antibody:

- **Anti-myelin basic protein (MBP):**

Rabbit polyclonal, 1:300 dilution, Abcam (ab40390), Cambridge, UK

After rinsing, slides were incubated with biotinylated secondary antibody, then streptavidin-HRP and 3,3'-diaminobenzidine (DAB) for 30 minutes. Counterstaining was performed with Mayer's hematoxylin. Slides were mounted and examined under an Olympus light microscope [20].

#### **Morphometric and statistical studies:**

At least five non-overlapping histological sections were estimated semi-quantitatively using image J analyzer software to estimate axon destruction and the G-ratio (axon diameter/ fiber diameter).

For IHC analysis, data obtained from different sections of rats were examined using ImageJ analyzer software to measure the percentage of immunopositive cells in the MBP immune stain.

#### **Statistical Analysis**

The Shapiro-Wilk test indicated that our data exhibited normal distribution. Also, Lavene's test indicated homogeneity of variance among groups. So, statistical comparisons among groups were made using one-way analysis of variance (ANOVA). All post hoc tests used Tukey's HSD, which maintains family-wise error rate (FWER) at  $\alpha = 0.05$  for the full set of comparisons. All data were expressed as mean  $\pm$  standard deviation (SD).

The confidence interval was 95%. The effect size was represented by Eta-squared ( $\eta^2$ ).  $\eta^2 = 0.01$  was considered small effect size,  $\eta^2 = 0.06$  was considered moderate effect size, and  $\eta^2 = 0.14$  was considered large effect size. Differences were considered statistically significant at  $P \leq 0.05$ . SPSS (Ver. 26.0, IBM Co. USA) was used for conducting statistical analysis.

#### **Results**

##### **ART ameliorated neurological and electrophysiological tests in ACR-induced neuropathy in rats**

**Fig.1a** illustrated that after conducting the hot plate test, the latency time of the ACR group was reduced compared to the control group ( $8.2 \pm 2.3$  s (95% CI: 5.47–10.93) vs.  $14.8 \pm 2.1$  s (95% CI: 12.39–17.21), respectively;  $P < 0.001$ ). Treatment with ART resulted in a marked increase in the latency time compared to the ACR group ( $11.8 \pm 1.63$  s (95% CI: 10.01–13.59),  $P < 0.001$ ). However, it remained lower than the control one ( $P = 0.032$ ). A considerable effect size was evident concerning hot plate test (0.722)

Also, our results showed that the NCV of the ACR group was attenuated compared to the control group ( $14.6 \pm 2.6$  m/s (95% CI: 11.59–17.61) vs.  $44.5 \pm 3.7$  m/s (95% CI: 40.27–48.73), respectively;  $P < 0.001$ ). ART therapy increased the conduction speed compared to the ACR group ( $33.6 \pm 3.3$  m/s (95% CI: 24.69–39.18),  $P < 0.001$ ). The ART group failed to elevate the NCV as the control group ( $P < 0.001$ ). A substantial effect size was observed for NCV (0.645) (**Fig.1b,c**).

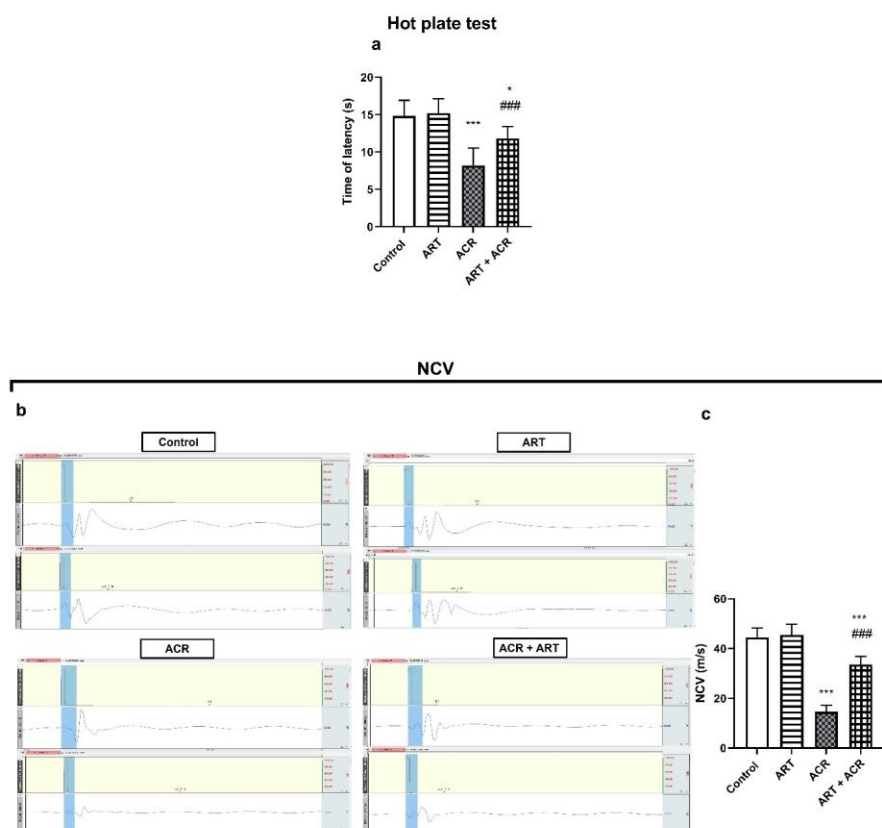


**Fig. 1** ART ameliorated neurological and electrophysiological tests in ACR-induced neuropathy in rats. (a) Hot plate test. (b) NCV image. (c) Mean NCV of the study groups. Mean  $\pm$  SD described the data ( $n = 8$ ). One-way ANOVA and Tukey tests interpreted the data. \* means  $P < 0.05$  and \*\*\* means  $P < 0.001$  vs the control group, ### means  $P < 0.001$  vs the ACR group. ACR = acrylamide; ART= artemisinin; NCV= nerve conduction velocity.

### ART ameliorated oxidative burden in ACR-induced neuropathy in rats.

ACR-induced neuropathy resulted in increased oxidative burden evidenced by elevated MDA and lowered TAC levels in comparison to the control group levels ( $10.3 \pm 2.2$  nmol/ml (95% CI: 7.76–12.83) and  $0.62 \pm 0.1$  mM/ml (95% CI: 0.51–0.73) vs.  $4.1 \pm 1.5$  nmol/ml (95% CI: 3.56–6.04) and  $2.6 \pm 0.18$  mM/ml (95% CI: 2.46–2.74);  $P < 0.001$ ). ART therapy exerted a noteworthy amelioration of oxidative burden confirmed by lowered MDA and elevated TAC levels compared to neuropathic animals ( $6.4 \pm 1.7$  nmol/ml (95% CI: 4.94–9.86) and  $2.1 \pm 0.14$  mM/ml (95% CI: 2.34–2.66), respectively;  $P < 0.001$ ). However, the ART-treated group's MDA levels remained higher than

the corresponding levels in the control group ( $P = 0.020$ ) while restoring TAC levels to normal ( $P = 0.083$ ). A large effect size was noted for MDA and TAC (0.639 and 0.982, respectively) (**Fig. 2a,b**).

### ART ameliorated inflammation in ACR-induced neuropathy in rats.

Neuropathy increased the inflammatory marker,  $\text{TNF-}\alpha$ , and decreased IL-10 level, which acts as an anti-inflammatory marker, compared to normal animals ( $48.8 \pm 5.3$  pg/ml (95% CI: 42.71–54.89) and  $9.6 \pm 2.1$  pg/ml (95% CI: 7.18–12.02) vs.  $20.6 \pm 5.1$  pg/ml (95% CI: 17.66–25.94) and  $18.8 \pm 3.6$  pg/ml (95% CI: 14.65–22.94), respectively;  $P < 0.001$ ). ART-treated rats manifested attenuation of  $\text{TNF-}\alpha$  and escalated IL-10 levels compared to neuropathic animals ( $35.2 \pm$



4.2pg/ml (95% CI: 30.38–39.99) and  $16.8 \pm 3.9$  pg/ml (95% CI: 12.32–21.28), respectively;  $P = 0.000$ ). ART restored IL-10 levels to normal ( $P = 0.620$ ); however, it failed to lower TNF- $\alpha$  values to normal control group values ( $P < 0.001$ ). The analysis demonstrated a large effect size concerning TNF- $\alpha$  and IL-10 levels (0.862 and 0.547, respectively)(Fig. 2c,d).

### ART ameliorated P13K/Akt expression in ACR-induced neuropathy in rats.

We found that neuropathic rats exhibited lower P13K and Akt expression levels than the control

ones ( $0.35 \pm 0.03$  (95% CI: 0.34–0.35) and  $0.48 \pm 0.05$  (95% CI: 0.47–0.48) vs.  $0.96 \pm 0.03$  (95% CI: 0.95–0.96) and  $0.98 \pm 0.09$  (95% CI: 0.97–0.98) respectively;  $P < 0.001$ ). ART could elevate P13K and Akt expression levels when compared to neuropathic rats ( $0.94 \pm 0.06$  (95% CI: 0.93–0.94) and  $0.96 \pm 0.08$  (95% CI: 0.95–0.96), respectively;  $P < 0.001$ ) and restore levels of these genes as compared to the control rats ( $P = 0.731$ ). A large effect size was detected regarding PI3K and Akt expression (1.000)(Fig. 2e,f)

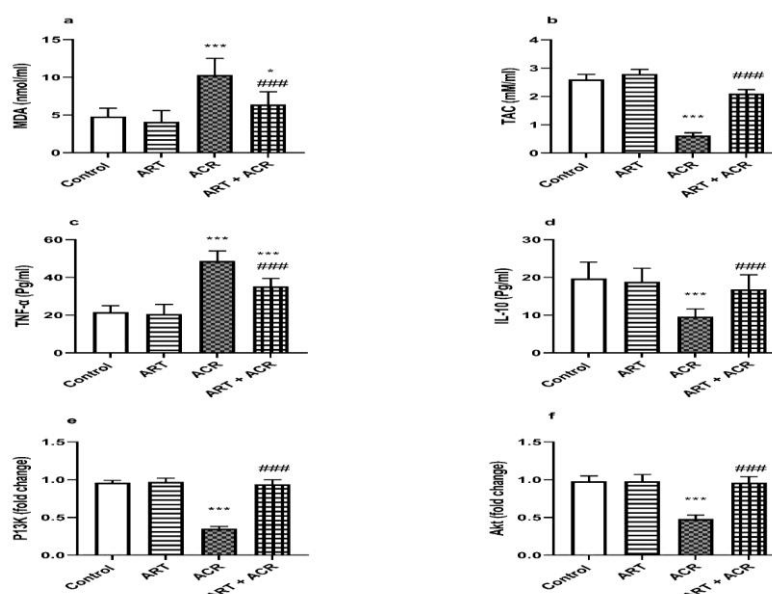


**Fig. 2 ART ameliorated oxidative burden, inflammation, and P13K/Akt expression in ACR-induced neuropathy in rats.** (a) MDA. (b) TAC. (c) TNF- $\alpha$ . (d) IL-10. (e) P13K. (f) Akt. Mean  $\pm$  SD described the data ( $n = 8$ ). One-way ANOVA and Tukey tests interpreted the data. \* means  $P < 0.05$  and \*\*\* means  $P < 0.001$  vs the Control group, ### means  $P < 0.001$  vs the ACR group. ACR = acrylamide; AKT = protein kinase B; ART = artemisinin; IL-10 = interleukin 10; MDA = malondialdehyde; P13K = Phosphatidylinositol-3-Kinase; TAC = total antioxidant capacity; TNF- $\alpha$  = tumor necrosis factor  $\alpha$ .

The control and ART groups' sciatic nerve sections displayed preserved myelin, regular arranged nerve axons and Schwann cells. Sciatic nerve section of the ACR group manifested markedly degenerated nerve axons with marked vacuolar degeneration with increased Schwann cells number in relation to decreased axons numbers. Sections of the ACR + ART group

exhibited marked improvement of nerve bundle and nerve axons and Schwann cells with increased myelination (Fig. 3).

Semi-quantitative analysis of histopathological examination revealed that axon destruction was increased in the ADR group compared to the control group ( $P < 0.001$ ). Treatment with ART reduced axon destruction compared to the ACR

group ( $P < 0.001$ ) and restored nerve axon to control group levels ( $P = 0.09$ ). A large effect size was detected regarding axon destruction (0.993) (Table 1).

The axon and nerve fiber diameters were eminently reduced in the neuropathic rats compared to normal ones ( $P < 0.001$ ). On the other hand, axon and nerve fiber diameters increased in response to ART therapy compared to neuropathic rats ( $P = 0.000$ ). ART therapy regained axon and nerve fiber diameters to control group values ( $P = 0.73$  and  $P = 0.46$ , respectively). A large effect

size was detected regarding the axon and nerve fiber diameters (0.277 and 0.739, respectively)(Table 1).

Conversely, the G ratio witnessed a noteworthy increase in the ACR-treated rats, indicating low nerve conduction velocity, compared to control rats ( $P < 0.001$ ). ART treatment reversed ACR's effect on the G ratio ( $P < 0.001$ ), restoring normal levels of the control group ( $P = 0.081$ ). A large effect size was detected regarding the G ratio (0.722)(Table 1).

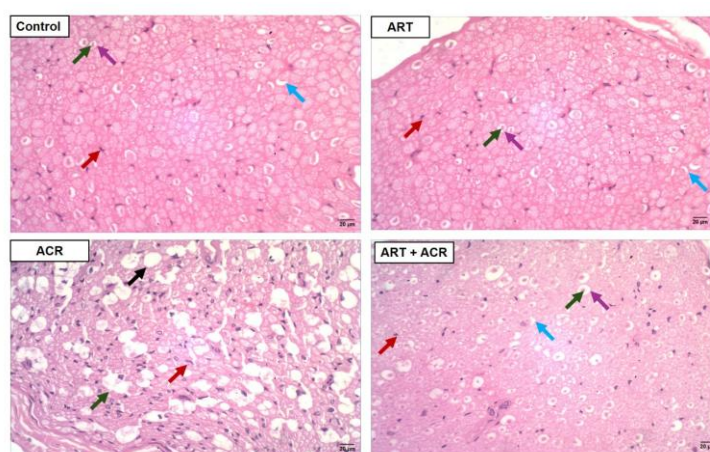


**Fig. 3 ART ameliorated histopathological changes in ACR-induced neuropathy in rats.** Sciatic nerve section of a normal rat in the control group showing preserved myelin (purple arrow), regular arranged nerve axons (green arrow) and Schwann cells (red arrow) (H&E,  $\times 400$ ). Sciatic nerve section of a rat in the ART group showing preserved myelin (purple arrow), regular arranged nerve axons (green arrow) and Schwann cells (red arrow), like the control group. Blood vessels are preserved (blue arrow) (H&E  $\times 400$ ). Sciatic nerve section of a rat in the ACR group showing markedly degenerated nerve axons (green arrow) with marked vacuolar degeneration (black arrow). Schwann cell numbers markedly decreased in relation to the decreased number of axons (red arrow)(H&E  $\times 400$ ). Sections of the ACR + ART group showing marked improvement of nerve bundle and nerve axons and Schwann cells (red arrow) with increased myelin (purple arrow). Blood vessels are preserved (blue arrow) (H&E  $\times 400$ ).

**Table 1. Analysis of histopathological examination.**

	Control	ART	ACR	ART + ACR
<b>Axon destruction</b>	0.0 $\pm$ 0.0 (95% CI: 0–0)	0.0 $\pm$ 0.0 (95% CI: 0–0)	3.1 $\pm$ 0.2 (95% CI: 2.84–3.32)***	0.3 $\pm$ 0.05(95% CI: 0.24–0.36) ###
<b>Axon Diameter (<math>\mu</math>m)</b>	12.8 $\pm$ 2.4(95% CI: 10.03–15.59)	13.6 $\pm$ 2.6(95% CI: 10.82–16.34)	9.9 $\pm$ 1.8(95% CI: 7.80– 12.09) ***	11.9 $\pm$ 2.5(95% CI: 9.51–14.22) ###
<b>Nerve fiber diameter (<math>\mu</math>m)</b>	24.6 $\pm$ 3.2(95% CI: 20.88–28.22)	26.8 $\pm$ 4.2(95% CI: 21.92–31.55)	13.9 $\pm$ 2.3(95% CI: 11.33–15.84)***	22.1 $\pm$ 1.9(95% CI: 19.89–24.21) ###
<b>G ratio</b>	0.52 $\pm$ 0.02(95% CI: 0.5–0.53)	0.51 $\pm$ 0.03(95% CI: 0.0.47–0.54)	0.71 $\pm$ 0.06(95% CI: 0.64–0.77) ***	0.53 $\pm$ 0.07(95% CI: 0.41–0.6) ###

Mean  $\pm$  SD described the data ( $n = 8$ ). One-way ANOVA and Tukey tests interpreted the data. \*\*\* means  $P < 0.001$ . vs the control group, ### means  $P < 0.001$  vs the ACR group. ACR = acrylamide; ART = artemisinin.



### ART ameliorated MBP expression in ACR-induced neuropathy in rats.

The mean value of MBP expression declined in the ACR group compared to the control group ( $20.0 \pm 2.8$  (95% CI: 16.78–23.22) vs.  $41.0 \pm 4.1$  (95% CI: 36.29–45.71), respectively;  $P < 0.001$ ). Conversely, the ART-treated group displayed a

notable increase in MBP expression compared to the ACR group ( $39.0 \pm 3.3$  (95% CI: 35.21–42.79),  $P < 0.001$ ) with attaining normal expression values of the control rats ( $P = 0.800$ ). A large effect size was detected regarding MBP expression (0.870) (Fig. 4).

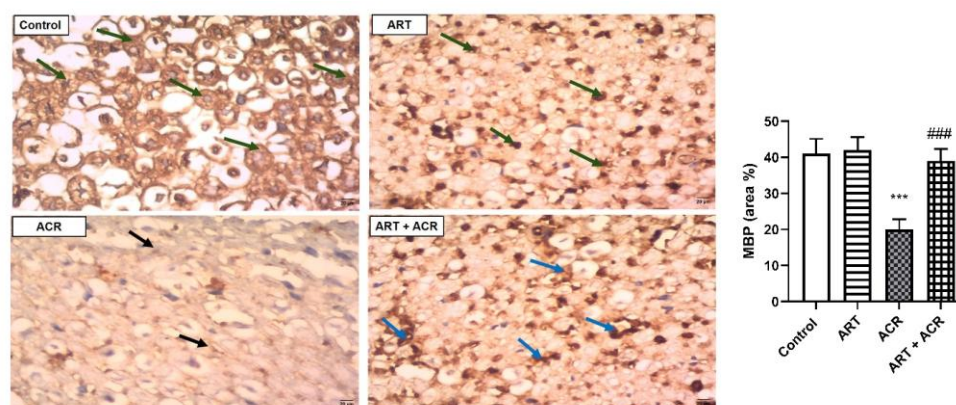


**Fig. 4** ART ameliorated MBP expression in ACR-induced neuropathy in rats. Representative MBP photos of different groups. The control and ART groups show excessive MBP expression (green arrows). The ACR group showing minimal MBP expression (black arrows). The ACR + ART group showing moderate MBP expression (blue arrows). (b) Mean MBP expression. Mean  $\pm$  SD described the data ( $n = 8$ ). One-way ANOVA and Tukey tests interpreted the data. \*\*\* means  $P < 0.001$  vs the control group, ### means  $P < 0.001$  vs the ACR group. ACR = acrylamide; ART = artemisinin; MBP = myelin basic protein.

### Discussion

Peripheral neuropathy resulting from exposure to environmental neurotoxins like acrylamide (ACR) continues to pose a significant biomedical challenge due to its multifactorial pathogenesis involving oxidative stress, neuroinflammation, and axonal degeneration. In this study, we examined the neuroprotective potential of artemisinin (ART) against ACR-induced peripheral neuropathy in rats. The findings of our investigation showed that ART significantly improved nerve conduction velocity (NCV), increased thermal latency in pain perception, restored antioxidant and anti-inflammatory balance, upregulated PI3K/Akt expression, and improved both histological nerve integrity and MBP expression.

ACR exposure led to a marked decrease in NCV and pain threshold as assessed by the hot plate test, indicative of peripheral nerve dysfunction. These findings corroborate those of Ersoy et al. [14], who reported functional deficits and structural damage in peripheral nerves of ACR-treated rats. The ability of ART to partially restore NCV and thermal latency is supported by Ji et al. [21], who demonstrated that ART improved neurobehavioral recovery in cerebral ischemia through the suppression of inflammatory signaling via the NF- $\kappa$ B pathway. However, our data also showed that ART did not fully restore NCV values to normal, indicating that while ART confers a protective effect, it may not completely reverse acrylamide-mediated nerve injury.

Oxidative stress plays a central role in ACR-induced neurotoxicity. Elevated MDA and reduced TAC levels in our ACR group are consistent with reports by Zhao et al. [5], who observed enhanced lipid peroxidation and redox imbalance in ACR-exposed models. Our study's reduction in MDA and restoration of TAC by ART further supports prior findings where ART exhibited antioxidant effects via Nrf2 signaling activation [22]. Nevertheless, the inability of ART to restore MDA levels to normal suggests persistent low-grade oxidative stress, similar to the residual damage described in earlier studies by Simon et al. [23], highlighting the importance of combination therapies.

Inflammatory markers such as TNF- $\alpha$  and IL-10 are pivotal mediators in ACR-induced neuroinflammation. We observed that ACR increased TNF- $\alpha$  and decreased IL-10, aligning with findings by Zhang et al. [24] who linked TNF- $\alpha$  upregulation to enhanced neuronal apoptosis. ART successfully reduced TNF- $\alpha$  and increased IL-10 levels in our study, indicating potent anti-inflammatory activity. Similar effects were observed by Oraebosi[25], who demonstrated ART's anti-inflammatory action in hepatic injury models via inhibition of pro-inflammatory cytokine expression. However, TNF- $\alpha$  levels in ART-treated rats did not return to baseline, suggesting partial suppression of inflammatory signaling, a limitation also noted in the study by Abo-Elsoud et al. [20] using pirfenidone.

At the molecular level, our data indicated significant downregulation of PI3K and Akt in ACR-exposed rats, which was reversed by ART treatment. This observation supports findings by Dai and Lu [26], who showed that ART alleviates

oxidative stress in trophoblastic cells by modulating the PI3K/Akt/mTOR pathway. This pathway is integral to regulating neuronal size, axon growth, and synapse, which is important for neuronal survival, growth, and regeneration. It plays a significant role in neuronal development, plasticity, and response to injury or stress, as confirmed by He et al. [27] in a model of hepatic ischemia-reperfusion injury. Also, Arthur et al. [28] demonstrated that ART could improve neurodegenerative disorders by modulating the PI3K/Akt/mTOR pathway with subsequent inhibition of oxidative stress, neuroinflammation, and apoptosis. Restoration of these signaling molecules suggests ART's ability to support neuronal survival and regeneration.

Histological evaluation revealed severe vacuolar degeneration, axonal disruption, and increased Schwann cell proliferation in the ACR group, all mitigated to varying extents in ART-treated animals. These findings align with those of Tang et al. [29], who reported improved neural structure and cellular regeneration following treatment with neurotrophic modulators. While ART substantially improved nerve architecture, the persistence of some pathological features underscores the necessity for longer treatment durations or adjunct therapies.

According to G-ratio evaluation, a key indicator of nerve fiber myelination and conduction velocity, ART showed a lower G ratio, indicating thick myelin and fast conduction velocity. These findings are in line with those of Chen et al. [30], who documented improved axon myelination and conduction velocity by treating ART. .

ART's impact on MBP expression—a key marker of myelin sheath integrity—was noteworthy. MBP

levels were significantly reduced in the ACR group and only partially restored by ART. These outcomes are consistent with the work of El Abo-Elsoud *et al.* [20], who documented reduced MBP in diabetic neuropathy models and partial improvement following antioxidant therapy. Guo *et al.* [31] also reported that ART upregulated MBP in neural regeneration by modulating the PI3K/Akt/mTOR axis, affirming the myelin-protective effect observed in our study.

While ART showed significant neuroprotective effects, it did not achieve full reversal of all biomarkers or functional parameters. This partial recovery suggests that ART might best serve as a multi-agent therapeutic strategy component. Pasha *et al.* [32] argued for the benefit of polytherapy in neuropathic disorders, especially in conditions where oxidative, inflammatory, and degenerative pathways intersect. Similarly, comparisons with pirfenidone [20] and curcumin [33] highlight the advantage of combining ART with agents having stronger anti-inflammatory or remyelination properties.

Future studies should also explore ART's long-term safety profile, its effects in female and aged animal models, and potential synergistic effects with existing neuroprotectants. Given the rising incidence of environmental toxin-induced neuropathies and the limited treatment options, ART holds promise as a valuable addition to the neurotherapeutic arsenal.

### Conclusion

Artemisinin (ART) demonstrated a promising neuroprotective role against acrylamide (ACR)-induced peripheral neuropathy in rats. ART treatment improves electrophysiological changes and pain threshold, suggesting functional

restoration, likely via its antioxidant and anti-inflammatory actions and upregulation of the PI3K/AKT gene expression, signifying stimulation of key survival and anti-apoptotic signaling pathways. Further studies are warranted to investigate its long-term efficacy, optimal dosing, and possible synergistic effects when combined with other neuroprotective agents.

### Author Contribution

Conceptualization: R.A.A.A.-E. and E.A.A.; Methodology: R.A.A.A.-E., E.O.I., E.A.A., A.S.A.A., M.E.T.; Formal Analysis (Statistical): R.A.A.A.-E. and E.A.A.; Investigation (Histopathological Examination): A.S.A.A.; Writing – Original Draft Preparation: R.A.A.A.-E., E.O.I., E.A.A., A.S.A.A., M.E.T.; Writing – Review & Editing: R.A.A.A.-E., E.O.I., E.A.A., A.S.A.A., M.E.T. All authors have read and agreed to the published version of the manuscript. The authors affirm that all data were produced internally, and no external paper-writing services were utilized.

**AI and plagiarism transparency:** We confirm that no AI-assisted writing was utilized in our research.

### Acknowledgement

We thank Dr. Mohamed S. Rizk for performing biochemical studies of this work.

### Competing Interest

The authors declare that they have no competing interests.

### Data availability statement

All data backing the present study's findings can be provided upon inquiry

### The data Funding

This research received no specific grant from funding agencies in the public, commercial, or not-for-profit sectors.

## References

1. **Bin-Jumah M, Abdel-Fattah AFM, Saied EM, El-Seedi HR, Abdel-Daim MM.** Acrylamide-induced peripheral neuropathy: manifestations, mechanisms, and potential treatment modalities. *Environ Sci Pollut Res Int.* 2021 Mar;28(11):13031–46. <https://doi.org/10.1007/s11356-020-12287-6>
2. **Jiang Y, Du H, Liu X, Fu X, Li X, Cao Q.** Artemisinin alleviates atherosclerotic lesion by reducing macrophage inflammation via regulation of AMPK/NF- $\kappa$ B/NLRP3 inflammasomes pathway. *J Drug Target.* 2020 Jan;28(1):70–9. <https://doi.org/10.1080/1061186X.2019.1616296>
3. **Zhao M, Zhang B, Deng L.** The Mechanism of Acrylamide-Induced Neurotoxicity: Current Status and Future Perspectives. *Front Nutr.* 2022;9:859189. <https://doi.org/10.3389/fnut.2022.859189>
4. **Rajeh NA.** Mechanistic progression of acrylamide neurotoxicity linked to neurodegeneration and mitigation strategies. *Discov Appl Sci [Internet].* 2024;6(4). <https://doi.org/10.1007/s42452-024-05850-0>
5. **Zhao M, Deng L, Lu X, Fan L, Zhu Y, Zhao L.** The involvement of oxidative stress, neuronal lesions, neurotransmission impairment, and neuroinflammation in acrylamide-induced neurotoxicity in C57/BL6 mice. *Environ Sci Pollut Res Int.* 2022 Jun;29(27):41151–67. <https://doi.org/10.1007/s11356-021-18146-2>
6. **Kopańska M, Łagowska A, Kuduk B, Banaś-Ząbczyk A.** Acrylamide Neurotoxicity as a Possible Factor Responsible for Inflammation in the Cholinergic Nervous System. *Int J Mol Sci.* 2022 Feb;23(4). <https://doi.org/10.3390/ijms23042030>
7. **Liu Y, Yan D, Wang Y, Zhang X, Wang N, Jiao Y, et al.** Subchronic exposure to acrylamide caused behaviour disorders and related pathological and molecular changes in rat cerebellum. *Toxicol Lett.* 2021 Apr;340:23–32. <https://doi.org/10.1016/j.toxlet.2021.01.009>
8. **Wang S, Song M, Yong H, Zhang C, Kang K, Liu Z, et al.** Mitochondrial Localization of SARM1 in Acrylamide Intoxication Induces Mitophagy and Limits Neuropathy. *Mol Neurobiol.* 2022 Dec;59(12):7337–53. <https://doi.org/10.1007/s12035-022-03050-8>
9. **Yan D, Dai L, Zhang X, Wang Y, Yan H.** Subchronic Acrylamide Exposure Activates PERK-eIF2 $\alpha$  Signaling Pathway and Induces Synaptic Impairment in Rat Hippocampus. *ACS Chem Neurosci.* 2022 May;13(9):1370–81. <https://doi.org/10.1021/acscchemneuro.1c00648>
10. **Eskut N, Koskderelioglu A.** Neurotoxic Agents and Peripheral Neuropathy. In: Sabuncuoglu S, editor. *Neurotoxicity [Internet].* Rijeka: IntechOpen; 2021.

- <https://doi.org/10.5772/intechopen.101103>
11. **Hu N, Liu J, Luo Y, Li Y.** A comprehensive review of traditional Chinese medicine in treating neuropathic pain. *Heliyon*. 2024 Sep;10(17):e37350. <https://doi.org/10.1016/j.heliyon.2024.e37350>
  12. **Arifin WN, Zahiruddin WM.** Sample size calculation in animal studies using resource equation approach. *Malaysian J Med Sci*. 2017;24(5):101–5. <https://doi.org/10.21315/mjms2017.24.5.11>
  13. **Gu Y, Wang X, Wu G, Wang X, Cao H, Tang Y, et al.** Artemisinin suppresses sympathetic hyperinnervation following myocardial infarction via anti-inflammatory effects. *J Mol Histol*. 2012 Dec;43(6):737–43. <https://doi.org/10.1007/s10735-012-9440-0>
  14. **Ersoy A, Tanoglu C, Yazici GN, Coban TA, Mammadov R, Suleyman H.** The Effect of Anakinra on Acrylamide-induced Peripheral Neuropathy and Neuropathic Pain in Rats. *Brazilian J Pharm Sci*. 2022;58:1–12. <https://doi.org/10.1590/s2175-97902022e21010>
  15. **Pennisi M, Malaguarnera G, Puglisi V, Vinciguerra L, Vacante M, Malaguarnera M.** Neurotoxicity of acrylamide in exposed workers. *Int J Environ Res Public Health*. 2013;10(9):3843–54. <https://doi.org/10.3390/ijerph10093843>
  16. **El Agamy D, Elseadawy R, El Tohamy M, Abdelaziz S, Abo-Elsoud R.** Serum uric acid as a biological marker for assessment of progression of glycemic status and polyneuropathy in experimentally induced type 2 diabetic rats. *Bull Egypt Soc Physiol Sci*. 2023;0(0):230–44. <https://doi.org/10.21608/besps.2023.204057.1138>
  17. **Huseyinoglu N, Ozaydin I, Huseyinoglu U, Yayla S, Aksoy O.** Minimally Invasive Motor Nerve Conduction Study of the Rat Sciatic and Tail Nerves. *Kafkas Univ Vet Fak Derg*. 2013;19(6):943–8. <https://doi.org/10.9775/kvfd.2013.9065>
  18. **Hüseyinoğlu N, Özaydin I, Yayla S, Yildirim CH, Aksoy Ö, Kaya M, et al.** Electrophysiological assessment of the effects of silicone tubes and hyaluronic acid on nerve regeneration in rats with sciatic neurorrhaphy. *Kafkas Univ Vet Fak Derg*. 2012;18(6):917–22. <https://doi.org/10.9775/kvfd.2012.6373>
  19. **Korte N, Schenk HC, Grothe C, Tipold A, Haastert-Talini K.** Evaluation of periodic electrodiagnostic measurements to monitor motor recovery after different peripheral nerve lesions in the rat. *Muscle Nerve*. 2011 Jul;44(1):63–73. <https://doi.org/10.1002/mus.22023>
  20. **Abo RAA, Eman E, Marwa AA, Gholam A Al, Rizk MS.** Pirfenidone mitigates demyelination and electrophysiological alterations in multiple sclerosis : Targeting NF -  $\kappa$ B , sirt1 , and neurotrophic genes. *Naunyn Schmiedebergs Arch Pharmacol [Internet]*. 2024;(0123456789). <https://doi.org/10.1007/s00210-024-03496-8>



21. **Ji H, Jin H, Li G, Jin L, Ren X, Lv Y, et al.** Artemisinin protects against cerebral ischemia and reperfusion injury via inhibiting the NF- $\kappa$ B pathway. *Open Med (Warsaw, Poland)*. 2022;17(1):871–81. <https://doi.org/10.1515/med-2022-0435>
22. **Long Z, Xiang W, Xiao W, Min Y, Qu F, Zhang B, et al.** Advances in the study of artemisinin and its derivatives for the treatment of rheumatic skeletal disorders, autoimmune inflammatory diseases, and autoimmune disorders: a comprehensive review. *Front Immunol*. 2024;15:1432625. <https://doi.org/10.3389/fimmu.2024.1432625>
23. **Simon AR, Rai U, Fanburg BL, Cochran BH.** Activation of the JAK-STAT pathway by reactive oxygen species. *Am J Physiol*. 1998 Dec;275(6):C1640–52. <https://doi.org/10.1152/ajpcell.1998.275.6.C1640>
24. **Zhang X, Deng S, Peng Y, Wei H, Tian Z.** ALKBH5 inhibits TNF- $\alpha$ -induced apoptosis of HUVECs through Bcl-2 pathway. *Open Med (Warsaw, Poland)*. 2022;17(1):1092–9. <https://doi.org/10.1515/med-2022-0484>
25. **Oraebosi MI.** Beneficial interaction between *Ficus platyphylla* and artesunate on cytokines TNF- $\alpha$  and IL-10 and oxidative stress in *Plasmodium berghei*-infected mice. *Ann Parasitol*. 2022;68(1):111–20. <https://doi.org/10.17420/ap6801.415>
26. **Dai H, Lu X.** MGST1 alleviates the oxidative stress of trophoblast cells induced by hypoxia/reoxygenation and promotes cell proliferation, migration, and invasion by activating the PI3K/AKT/mTOR pathway. *Open Med (Warsaw, Poland)*. 2022;17(1):2062–71. <https://doi.org/10.1515/med-2022-0617>
27. **He X, Li Y, Deng B, Lin A, Zhang G, Ma M, et al.** The PI3K/AKT signalling pathway in inflammation, cell death and glial scar formation after traumatic spinal cord injury: Mechanisms and therapeutic opportunities. *Cell Prolif*. 2022 Sep;55(9):e13275. <https://doi.org/10.1111/cpr.13275>
28. **Arthur R, Navik U, Kumar P.** Repurposing artemisinins as neuroprotective agents: a focus on the PI3k/Akt signalling pathway. *Naunyn Schmiedebergs Arch Pharmacol*. 2023 Apr;396(4):593–605. <https://doi.org/10.1007/s00210-022-02350-z>
29. **Tang Z, Yang C, He Z, Deng Z, Li X.** Notoginsenoside R1 alleviates spinal cord injury through the miR-301a/KLF7 axis to activate Wnt/ $\beta$ -catenin pathway. *Open Med*. 2022;17(1):741–55. <https://doi.org/10.1515/med-2022-0461>
30. **Chen S, Wu L, He B, Zhou G, Xu Y, Zhu G, et al.** Artemisinin Facilitates Motor Function Recovery by Enhancing Motoneuronal Survival and Axonal Remyelination in Rats Following Brachial Plexus Root Avulsion. *ACS Chem Neurosci*. 2021 Sep;12(17):3148–56. <https://doi.org/10.1021/acchemneuro.1c00120>

- 
31. **Guo F, Qin X, Mao J, Xu Y, Xie J.** Potential Protective Effects of Pungent Flavor Components in Neurodegenerative Diseases. *Molecules*. 2024 Dec;29(23). <https://doi.org/10.3390/molecules29235700>
  32. **Pasha R, Azmi S, Ferdousi M, Kalteniece A, Bashir B, Gouni-Berthold I, et al.** Lipids, Lipid-Lowering Therapy, and Neuropathy: A Narrative Review. *Clin Ther*. 2022 Jul;44(7):1012–25. <https://doi.org/10.1016/j.clinthera.2022.03.013>
  33. **Caillaud M, Aung Myo YP, McKiver BD, Osinska Warncke U, Thompson D, Mann J, et al.** Key Developments in the Potential of Curcumin for the Treatment of Peripheral Neuropathies. *Antioxidants*. 2020 Oct;9(10). <https://doi.org/10.3390/antiox9100950>